# Variable-property effects in free convection

**A. Pozzi and M. Lupo**
Istituto di Gasdinamica, Facoltá di Ingegneria, University of Naples, Italy

An analysis is presented of the effects of variable properties on the thermo-fluid-dynamic field in natural convection along a vertical flat plate of nonzero thickness whose outer surface is at constant temperature. Viscosity and thermal conductivity are assumed to depend on temperature in a polynomial form. The method of solution of the problem, which is not governed by similarity solutions because of the nonzero thickness of the plate, is based on two expansions coupled through an application of Padé-approximant techniques. The method is applied to natural convection of air over several temperature ranges. The influence on the thermo-fluid-dynamic field of the law of variation of viscosity and thermal conductivity is discussed.

**Keywords:** natural convection; variable-property effects

## Introduction

Analysis of natural convection problems is usually performed by applying the Boussinesq approximation, which consists of considering all the properties constant except density when it appears in the buoyancy term of the equation of motion. Some empirical methods, such as the reference-temperature method and the property-ratio method (see, e.g., Kays[1]) have been proposed to evaluate the effects of variable properties on the thermo-fluid-dynamic field.

In the reference-temperature method, the problem is still solved within the Boussinesq approximation but the properties are calculated at a reference temperature $T_r = T_w - r(T_w - T_\infty)$, in which $r$ is an empirical coefficient that is different for each property. In the property-ratio method, the variable-property results are obtained by multiplying the corresponding constant-property results by a factor of the form $\Pi[\alpha_i(T_w)/\alpha_i(T_\infty)]^{n_i}$, where $\alpha_1 = \mu$, $\alpha_2 = \lambda$, $\alpha_3 = \rho$ and the exponents $n_i$ are determined empirically.

Sparrow and Gregg[2] used the first method and found the value of 0.38 for $r$ convenient for calculating the Nusselt number for several classes of gases. Minkowycz and Sparrow[3] used the value of 0.46 for steam. Fujii *et al.*[4] suggested the value of 0.25 for liquids.

Recently, the problem of variable-property effects has been studied for heat transfer at walls of zero thickness for the case of small temperature differences. In particular, Carey and Mollendorf[5] presented a first-order perturbation analysis for liquids, in which they assumed a linear dependence of viscosity on temperature. Gray and Giorgini[6] analyzed the limits of applicability of the Boussinesq approximation.

Merker and Mey,[7] studying natural convection in a shallow cavity, found that the reference temperature can be assumed to be the arithmetic mean of the highest and lowest temperature, if the difference of these temperatures is on the order of 30 K or less. Variable-property effects in internal flows were studied by Herwig[8] (in circular pipes) and by Herwig and Klemp[9] (in annular pipes) by linear perturbation analysis.

In this study we addressed the problem of variable-property effects in free convection along a vertical flat plate without limitations on the difference between the wall and outer temperature, while also taking into account the influence of the thickness of the plate.

Address reprint requests to Professor Pozzi at the Istituto di Gasdinamica, Facoltá di Ingegneria, University of Naples, 80-80125 Naples, Italy.

Received 3 January 1989; accepted 23 October 1989

## Analysis of the problem

The steady two-dimensional (2-D) flow resulting from laminar natural convection along a side of a vertical flat plate is governed by the boundary layer equations, in which the buoyancy term $g(\rho_\infty - \rho)$ appearing in the equation of motion is usually written as $g\beta\rho(T - T_\infty)$, where $\beta$ is the coefficient of thermal expansion and, for a perfect gas, is equal to $1/T_\infty$.

Hence the dimensionless boundary layer equations governing the problem are

$$(\rho u)_x + (\rho v)_y = 0 \tag{1}$$

$$\rho(uu_x + vu_y) = (\mu u_y)_y + \rho\vartheta \tag{2}$$

$$\rho(u\vartheta_x + v\vartheta_y) = \frac{(\lambda\vartheta_y)_y}{\mathrm{Pr}} \tag{3}$$

where $\vartheta = (T - T_\infty)/(T_b - T_\infty)$ and Pr is the Prandtl number.

The reference frame is illustrated in Figure 1, where $b$ denotes the thickness of the plate, which is insulated on the edges, and a temperature $T_b$ is maintained on the side away from the fluid.

The reference quantities are: $L = v_\infty^{2/3}/g^{1/3}$ for $x'$, $L/d^{1/4}$ for $y'$, $\rho_\infty$ for $\rho$, $\mu_\infty$ for $\mu$, $\lambda_\infty$ for $\lambda$, and $v_\infty d^{1/4}$ for the stream function $\psi(\rho u = \psi_y\rho_\infty, \rho v = \psi_x\rho_\infty)$, where $d = \beta(T_b - T_\infty)$.

Equations 1–3 are usually solved using the Boussinesq approximation. It is possible to take into account the variable-property effects by means of the nondimensional Stewartson–Dorodnitzin transformation:

$$\xi = x \qquad \eta = \int_0^y \rho\, dy \tag{4}$$

assuming that the viscosity and thermal conductivity coefficients are proportional to absolute temperature, so that $\mu\rho = \lambda\rho = 1$.

This hypothesis concerning the dependence on temperature of the viscosity and thermal conductivity coefficients cannot be adequate to describe the thermo-fluid-dynamic field if the fluid-side plate temperature is very different from that of the outer side. Therefore we assume the following dependence of $\mu$ and $\lambda$ on absolute temperature $T$

$$\mu = \sum_{i=1}^{n} \alpha_i T^i \tag{5}$$

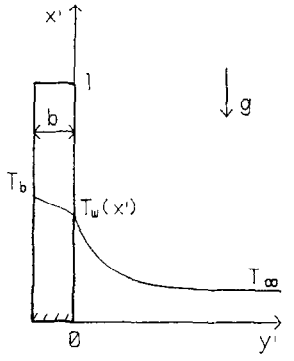


*Figure 1* Thermal model of a plate

$$\lambda = \sum_{i=1}^{n} \beta_i T^i \tag{6}$$

so that, in dimensionless form, the products $\mu\rho$ and $\lambda\rho$ ($\rho = 1/T$) are expressed by means of polynomials in terms of $\vartheta$:

$$\mu\rho = 1 + \sum_{i=1}^{n-1} a_i \vartheta^i \tag{7}$$

$$\lambda\rho = 1 + \sum_{i=1}^{n-1} b_i \vartheta^i \tag{8}$$

In particular, for $n=2$ we have

$$\mu\rho = 1 + a_1\vartheta \tag{7a}$$

$$\lambda\rho = 1 + b_1\vartheta \tag{8a}$$

where $a_1 = \alpha_2(T_b - T_\infty)/(\alpha_1 + \alpha_2 T_\infty)$ and

$b_1 = \beta_2(T_b - T_\infty)/(\alpha_1 + \alpha_2 T_\infty)$

Then Equations 1, 3, 7, and 8 give

$$u_x + V_\eta = 0 \tag{9}$$

$$uu_x + Vu_\eta = \left[\left(1 + \sum_{i=1}^{n-1} a_i \vartheta^i\right)\mu_\eta\right]_\eta + \vartheta \tag{10}$$

$$u\vartheta_x + V\vartheta_\eta = \frac{\left[\left(1 + \sum_{i=1}^{n-1} b_i \vartheta^i\right)\vartheta_\eta\right]_\eta}{\mathrm{Pr}} \tag{11}$$

where $V = \rho v + u\eta_x$.

The boundary conditions associated with Equations 9–11 are

$$u(x,0) = v(x,0) = u(x,\infty) = \vartheta(x,\infty) = 0 \tag{12}$$

$$u(0,\eta) = \vartheta(0,\eta) = 0 \tag{13}$$

The boundary condition of Equation 13 usually involves assigning the temperature or the heat flux at the solid–fluid interface ($y=0$). For a plate of nonzero thickness, we must solve the coupled thermal fields in both the solid and the fluid. The coupling conditions require that the temperature and the heat flux be continuous at the interface.

The temperature $T_{so}$ in the solid, neglecting the wall's longitudinal conduction, is

$$T_{so} = T_w(x') - \frac{[T_b - T_w(x')]\,y'}{b}$$

where $T_w(x') = T(x', 0)$ is the unknown temperature at the interface.

The heat flux continuity condition, using Equation 8, may be written in dimensionless form as

$$p\left(1 + \sum_{i=1}^{n-1} b_i \vartheta_w^i\right)\vartheta_\eta(x,0) = \vartheta_w - 1 \tag{14}$$

## Notation

| | |
|---|---|
| $a_1$ | Coefficient in Equation 7 |
| $b$ | Plate thickness |
| $b_1$ | Coefficient in Equation 8 |
| $c_f$ | Friction coefficient, $\tau_w/\rho_\infty(v_\infty/x')^2$ |
| $d$ | $\beta(T_b - T_\infty)$ |
| $f_i$ | Functions occurring in the asymptotic expansion of $\psi$ |
| $g$ | Acceleration due to gravity |
| $g_i$ | Functions occurring in the initial expansion of $\psi$ |
| $\mathrm{Gr}_l$ | Grashof number referred to the length of the plate, $gdl^3/v^2$ |
| $\mathrm{Gr}_x$ | Grashof number referred to the abscissa $x'$, $gdx'^3/v^2$ |
| $h_i$ | Functions occurring in the initial expansion of $\vartheta$ |
| $K$ | Coefficient in the coupling parameter, $\lambda_{so} l/\lambda_\infty b$ |
| $l$ | Length of the plate |
| $L$ | Reference length, $v^{2/3}/g^{1/3}$ |
| $m$ | Expansion parameter in asymptomatic solution, $px^{-1/4}$ |
| $m_1$ | Expansion parameter in initial solution, $x^{1/5}/p^{4/5}$ |
| $\mathrm{Nu}_x$ | Nusselt number referred to the abscissa $x'$, $x'q_w(x')/\lambda_\infty(T_w - T_\infty)$ |
| $p$ | Coupling parameter, $d^{1/4}b\lambda_\infty/L\lambda_{so}$ |
| Pr | Prandtl number |
| $q_w$ | Wall heat flux |
| $s$ | Similarity variable for the initial expansion, $\eta/(px)^{1/5}$ |
| $T$ | Temperature |
| $T_b$ | Temperature at outside surface of the plate |
| $u, v$ | Velocity components |
| $x', y'$ | Dimensional cartesian coordinates, as indicated in Figure 1 |
| $x, y$ | Dimensionless cartesian coordinates |
| $z$ | Similarity variable for the asymptotic expansion, $\eta/x^{1/4}$ |

*Greek symbols*

| | |
|---|---|
| $\beta$ | Volume thermal expansion coefficient |
| $\vartheta$ | Dimensionless temperature $(T - T_\infty)/(T_b - T_\infty)$ |
| $\vartheta_i$ | Functions occurring in the asymptotic expansion of $\vartheta$ |
| $\lambda$ | Thermal conductivity |
| $\mu$ | Absolute viscosity |
| $\nu$ | Kinematic viscosity |
| $\rho$ | Fluid density |
| $\psi$ | Stream function |
| $\xi$ | New dimensionless abscissca, $x$ |
| $\eta$ | New dimensionless ordinate, $\int_0^y \rho\, dy$ |

*Subscripts*

| | |
|---|---|
| $so$ | Solid |
| $w$ | Solid–fluid interface conditions |
| $\infty$ | Ambient conditions |

where

$$p=\frac{d^{1/4}b\lambda_\infty}{L\lambda_{so}} \tag{15}$$

and $\lambda_{so}$ is the (constant) solid thermal conductivity. Equation 14 represents the last boundary condition associated with Equations 9–11.

## Solution method

Owing to the nonzero thickness of the plate, the problem does not allow use of similarity solutions; in fact the solution has a different character for low and high values of $x$. Therefore Equations 9–14 are solved by means of two expansions, reflecting the fact that the solution tends toward the isothermal one for $x\to\infty$ and toward the isoflux one for $x\to 0$.

In order to analyze the problem for high values of $x$, we assume (as a convenience) that $m=p/x^{1/4}$ and $z=\eta/x^{1/4}$ are independent variables. It is not possible to expand the unknowns in a MacLaurin series with respect to $m$ ($m\to 0$ corresponds to $x\to\infty$) because, although no problem is encountered for the first four coefficients, the equation that should determine the fifth one has no solution. Moreover, since $m$ diverges for $x$ vanishing, this series cannot satisfy any initial conditions. Therefore the asymptotic expansion must include nonintegral powers and logarithmic terms: In this way it is possible to satisfy conditions at a suitable point $x_0>0$. Nevertheless, as such terms do not appear below order 4,[10] they can be neglected in the procedure proposed.

In order to analyze the problem for small values of $x$ we (again for convenience) assume that $m_1=x^{1/5}/p^{4/5}$ and $s=\eta/(px)^{1/5}$ are independent variables. In this case it is possible to expand the unknowns in a MacLaurin series with respect to $m_1$ ($m_1=0$ for $x=0$). This expansion, the leading term of which represents the isoflux condition, has a finite radius of convergence and does not allow us to describe the entire thermo-fluid-dynamic field. The expansion does provide, if necessary, the initial conditions at $x_0$ for the asymptotic expansion. However, we show that it is possible, using Padé approximant techniques, not only to calculate the radius of convergence of the initial expansion, but also to obtain a representation valid over the whole field.

Every term of the two expansions is obtained by solving numerically a system of ordinary differential equations obtained in the usual way from Equations 9–14, applying Cauchy's rule for multiplication of power series. In particular, we assume (for the sake of simplicity) Equations 7a and 8a ($n=2$) for $\mu\rho$ and $\lambda\rho$. The method proposed works well also if the number of equations is large. Considering 11 and 4 terms for the initial and asymptotic expansions, respectively, is sufficient to obtain accurate results.

### *Expansion for high* x

To obtain the asymptotic expansion we introduce the same similarity variable used for the isothermal problem, $z=\eta/x^{1/4}$. We let $\psi=x^{3/4}f(x,z)$ and

$$m=\frac{p}{x^{1/4}} \tag{16}$$

If we expand the functions $f$ and $\vartheta$ in a MacLaurin series, writing

$$f=\sum_{i=0}^{\infty} m^i f_i(z) \quad\text{and}\quad \vartheta=\sum_{i=0}^{\infty} m^i\vartheta_i(z) \tag{17}$$

from Equations 7a, 8a, 10, 11, and 14, we find at the leading order the following system:

$$(1+a_1\vartheta_0)f_0'''+\left(a_1\vartheta_0'+\frac{3}{4}f_0\right)f_0''-\frac{1}{2}f_0'^2+\vartheta_0=0 \tag{18a}$$

$$(1+b_1\vartheta_0)\vartheta_0''+b_1\vartheta_0'^2+\frac{3}{4}\Pr f_0\vartheta_0'=0 \tag{18b}$$

$$f_0(0)=f_0'(0)=f_0'(\infty)=0 \tag{18c}$$

$$\vartheta_0(0)=1 \quad\text{and}\quad \vartheta_0(\infty)=0 \tag{18d}$$

(representing the isothermal problem) and at the $i$th order

$$(1+a_1\vartheta_0)f_i'''+\vartheta_i+a_1(\vartheta_i f_0''+\vartheta_0' f_i''+\vartheta_i' f_0'')-f_0' f_i'+\frac{3}{4}\left(f_0 f_i''+f_i f_0''\right)+\frac{i}{4}(f_i' f_0'-f_i f_0'')=S_i \tag{19a}$$

$$(1+b_1\vartheta_0)\vartheta_i''+b_1(\vartheta_i\vartheta_0''+2\vartheta_i'\vartheta_0')+\frac{3}{4}\Pr(f_0\vartheta_i'+f_i\vartheta_0')+\frac{i}{4}\Pr(\vartheta_i f_0'-f_i\vartheta_0')=T_i \tag{19b}$$

$$f_i(0)=f_i'(0)=f_i'(\infty)=0 \tag{19c}$$

$$\vartheta_i(0)=\vartheta_{i-1}'(0)+b_1A_{i-1}; \qquad \vartheta_i(\infty)=0 \tag{19d}$$

where

$$A_i=\sum_{j=0}^{i}\vartheta_j(0)\vartheta_{i-j}'(0)$$

$$S_i=\sum_{j=1}^{i-1}\left[\frac{1}{2}f_j'f_{i-j}'-\frac{3}{4}f_jf_{i-j}''-\frac{j}{4}(f_j'f_{i-j}'-f_jf_{i-j}'')-a_1(\vartheta_jf_{i-j}'''+\vartheta_j'f_{i-j}'')\right]$$

$$T_i=\sum_{j=1}^{i-1}\left[-b_1(\vartheta_j\vartheta_{i-j}''+\vartheta_j'\vartheta_{i-j}')-\frac{j}{4}\Pr(\vartheta_jf_{i-j}'+f_j\vartheta_{i-j}')-\frac{3}{4}\Pr f_j\vartheta_{i-j}'\right]$$

Equations 19 may be solved numerically without difficulty for $i=1$, 2, and 3; for $i=4$, Equations 19a and b, with $S_i=T_i=0$ and with the initial conditions $f_4(0)=f_4'(0)=\vartheta_4(0)=0$; $f_4''(0)=Cf_0''(0)$; $\vartheta_4'(0)=-C\vartheta_0'(0)$, where $C$ is a free constant, allows a solution by $f_4=C(3f_0-zf_0')$; $\vartheta_4=-Cz\vartheta_0'$, which satisfies the conditions at infinity $f_4'(\infty)=\vartheta_4(\infty)=0$. Therefore $f_4$ and $\vartheta_4$ represent an eigensolution of Equations 19.

To take into account terms of $0(m^4)$, we must modify the form of Equations 17 to include the eigensolutions and give initial conditions at $x=x_0>0$. However, we need to consider only the first four terms in Equation 17, because the Padé-approximant techniques permit us to obtain a representation valid in the entire thermo-fluid-dynamic field. Thus the asymptotic solution will check only the accuracy of the Padé representation at high values of $x$.

### *Expansion for low* x

Let $s=\eta/(px)^{1/5}$, $\psi=x^{4/5}g(x,s)/p^{1/5}$, $\vartheta=x^{1/5}h(x,s)/p^{4/5}$, and

$$m_1=\frac{x^{1/5}}{p^{4/5}} \tag{20}$$

We can expand the functions $g$ and $h$ in a MacLaurin series with respect to $m_1$, to get

$$g=\sum_{i=0}^{\infty} m_1^i g_i(s) \quad\text{and}\quad h=\sum_{i=0}^{\infty} m_1^i h_i(s) \tag{21}$$

In this way, if we assume that $g_i'(\infty)=h_i(\infty)=0$, the initial

conditions of Equation 13 are satisifed as well. If $x_0$ is a point of convergence of Equation 21, we can obtain in this point the initial conditions for a correct expansion in terms of $m$ (asymptotic expansion).

Equations 7a, 8a, 10, 11, and 14 give, as in the previous case, the equations to be used to calculate the functions $g_i(s)$ and $h_i(s)$ for any $i$. We can calculate the radius of convergence of Equations 21 by means of Padé-approximant techniques, after determining numerically the functions $g_i(s)$ and $h_i(s)$; at the same time, we shall obtain a new representation of the functions $g$ and $h$. The idea of Padé summation is to replace a power series $\sum a_n t^n$ by a sequence of rational functions of the form

$$P_M^N(t)=\frac{\sum_{n=0}^{N} A_n t^n}{\sum_{n=0}^{M} B_n t^n}$$

where $B_0$ may be set equal to 1 without loss of generality. The remaining $M+N+1$ coefficients, $A_n$ and $B_n$, may be chosen so that the first $M+N+1$ terms in the Taylor series expansion of $P_M^N(t)$ match the first $M+N+1$ terms of the power series $\sum_{n=0}^{\infty} a_n t^n$. The resulting rational function $P_M^N(t)$ is called a Padé approximant of functions $P_M^N$ for which $M=N$ is called the diagonal sequence.

In this way we can obtain rapid convergence by using only a few terms of the original Taylor series. Above all, the utility of Padé approximants lies in the fact that they also work well when the Taylor series does not converge.

The improvement with respect to the MacLaurin expansion obtained with Padé approximants is remarkable; in fact, the latter even matches the expansion for $x\to\infty$ very well, whereas the former diverges there. We demonstrate these effects and present all our results using Padé techniques.

## Results and discussion

We will apply the preceding analysis to the case of air (Pr=0.7), assuming for the ambient temperature, $T_\infty$, the value of 300 K and for $T_b$ the values of 700, 1000, and 1300 K ($d=\beta(T_b-T_\infty)=$ 1.33, 2.33, and 3.33). In these ranges we can well describe the variation of viscosity and thermal conductivity, utilizing Equations 5 and 6 and calculating coefficients so that the curves of $\mu$ and $\lambda$ pass respectively through $\mu(T_\infty)=184\times10^{-6}$ P and $\mu(T_b)=331$, 419, and $494\times10^{-6}$ P, and through $\lambda(T_\infty)=2.64\times10^{-2}$ W/mK and $\lambda(T_b)=5.16$, 6.78, and $8.37\times10^{-2}$ W/mK (see ref. 11). In this way the maximum error obtained for $\mu(T)$ and $\lambda(T)$ is only a few per cent.

We consider a plate of finite thickness $b$ and length $l$ and define a Grashof number $\mathrm{Gr}_l$ according to this length. Moreover, letting $K=\lambda_{so}l/\lambda_\infty b$, we can write $p=d^{1/4}/K$, $m=\mathrm{Gr}_l^{1/4}/(x'/l)^{1/4}K$ and $m_1=K^{4/5}(x'/l)^{1/5}/\mathrm{Gr}_l^{1/5}$. All results are obtained for $\mathrm{Gr}_l=10^9$ and for Pr=0.7.

The Padé-approximant technique used to calculate the radius of convergence of the original MacLaurin expansion for a coupled laminar convection–conduction problem[10] was also used for the representation of the functions. Thus we find that the MacLaurin-expansion Equations 21, have a finite radius of convergence (on the order of magnitude of unity (i.e., $m_1=0(1)$), whereas the Padé representation is valid for the entire field.

These results are shown in Figures 2 and 3, where $\vartheta_w$ is plotted versus $x'/l$ for the range 300–1000 K and for $K=250$. The asymptotic and initial expansion are evaluated with 4 and 11 terms, respectively.

Figure 2 shows that the initial expansion that coincides with Padé representation for $x'/l<0.1$ diverges when $x'/l>0.1$.

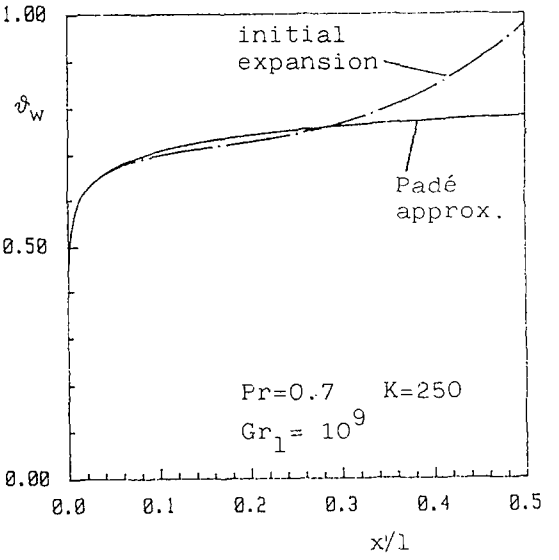


*Figure 2* Nondimensional temperature at the wall, $\vartheta_w$, given by initial expansion and Padé approximant

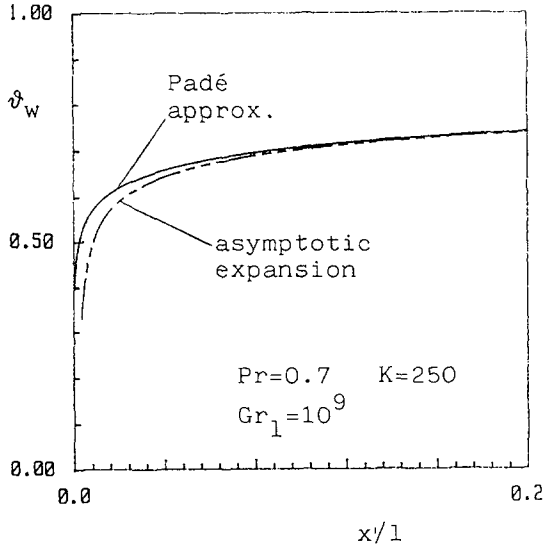


*Figure 3* Nondimensional temperature at the wall, $\vartheta_w$, given by asymptotic expansion and Padé approximant

Figure 3 shows that for $x'/l>0.1$ the Padé approximant and the asymptotic expansion give practically the same values ($x'/l=0.1$ corresponds to a value of $m_1$ close to the radius of convergence). Therefore Padé representation is valid also when the MacLaurin original expansion (initial expansion) does not converge. Hence Padé approximants accurately represent both low and high values of the abscissa.

In Figures 4–10, we denote the range 300–700 K by ——, the range 300–1000 K by – – – – and the range 300–1300 K by —·—; we denote the approximation $\mu\rho=\lambda\rho=1$ by ——.

We analyze the effects of the variable fluid properties and of the thickness of the plate on $\mathrm{Nu}_x$, $\vartheta_w$, and $c_f$, and temperature and velocity profiles. The Nusselt number, defined as $\mathrm{Nu}_x=x'q_w/\lambda_\infty(T_w-T_\infty)=-x'\lambda_w T_{y,w}/\lambda_\infty(T_w-T_\infty)$, is plotted in Figure 4 versus $x'/l$ for $K=250$. For the evaluation of the Nusselt number, the assumption $\mu\rho=\lambda\rho=1$ for air works well enough in the ranges of temperature considered. In fact, at $x/l=1.0$,

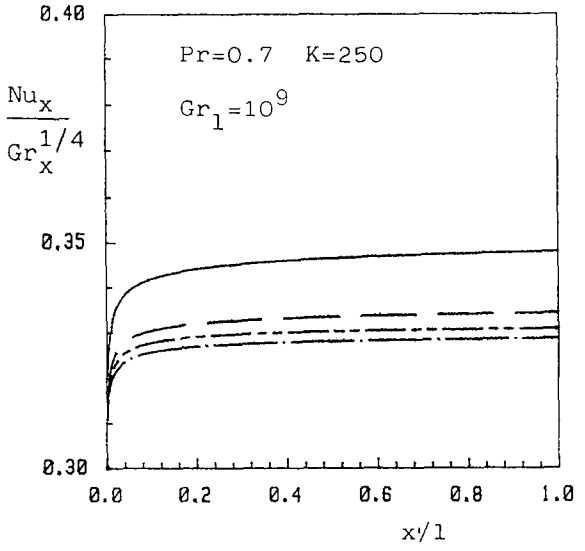


*Figure 4* Comparison of $Nu_x/Gr_x^{1/4}$ for $K=250$, for $d=1.33$, 2.33, and 3.33, with that of $\mu\rho=\lambda\rho=1$

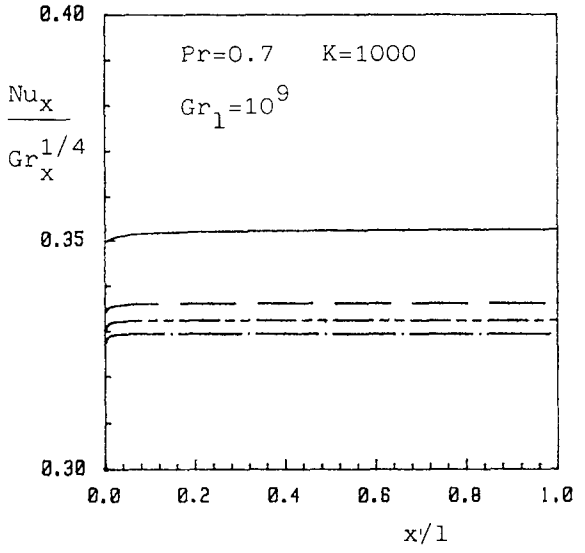


*Figure 5* Comparison of $Nu_x/Gr_x^{1/4}$ for $K=1000$, for $d=1.33$, 2.33, and 3.33, with that of $\mu\rho=\lambda\rho=1$

the difference is only about 4% in the range 300–700 K and about 6% in the range 300–1300 K. Considering a higher value of $K$, which corresponds to a smaller thermal resistance of the solid, does not modify these differences substantially.

In Figure 5 the curves of $Nu_x/Gr_x^{1/4}$ are based on $K=1000$. The difference is about 4.5% in the range 300–700 K and about 6.5% in the range 300–1300 K. In this case the curves are flatter than those in Figure 4, because for high values of $K$ the largest part of the variation in wall temperature is confined to a small region near the leading edge of the plate. Thus the wall–fluid interface can be considered almost completely isothermal.

The dimensionless wall temperature $\vartheta_w$ is plotted versus $x'/l$ in Figure 6 for $K=250$ and $K=1000$. Comparison of the curves of $\vartheta_w$, calculated with the assumption $\mu\rho=\lambda\rho=1$, to those in the range 300–1300 K shows that the dimensionless temperature at the wall is slightly dependent on the variation of $\mu$, $\lambda$, and $\rho$ with temperature. We found empirically for air that, in the ranges of temperature considered, we can obtain $Nu_x/Gr_x^{1/4}$ from the constant-property solution by calculating $\mu$ and $\lambda$ at the reference temperature $T_r=T_w-0.15(T_w-T_\infty)$. The results obtained for the range 300–1000 K are represented in Figure 7 by curve (*). Naturally, the most appropriate reference temperature is different for different quantities of interest ($c_f$, boundary layer thickness, flow rate).

The friction coefficient $c_f$, defined as $\tau_w/\rho_\infty(v_\infty/x')^2$, is plotted in Figure 8 for $d=1.33$ and $d=3.33$. The difference with respect to the curves obtained by using the assumption $\mu\rho=\lambda\rho=1$ (solid curves) is about 8% for $d=1.33$ and about 14% for $d=3.33$.

Padé-approximant techniques may also be used for determining temperature and velocity profiles. In fact, if we set $\sum_{i=0}^{N+M} m_1^i h_i(s)=\sum_{i=0}^{N} A_i m_1^i / \sum_{i=0}^{M} B_i m_1^i$, the Padé coefficients $A_i$ and $B_i$ would depend on $s$. By computing these coefficients for several values of $s$, we can draw temperature and velocity profiles for each value of $m_1$, that is, for each value of $x'/l$, as $m_1=K^{4/5}(x'/l)^{1/5}/Gr_l^{1/5}$.

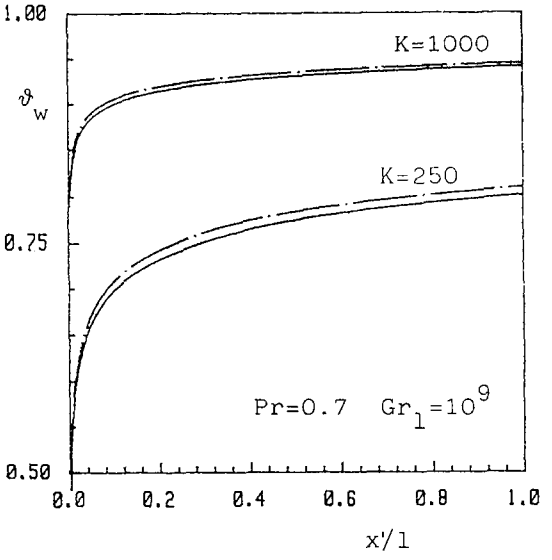


*Figure 6* Comparison of $\vartheta_w$ for $K=250$ and $K=1000$, for $d=3.33$, with that of $\mu\rho=\lambda\rho=1$

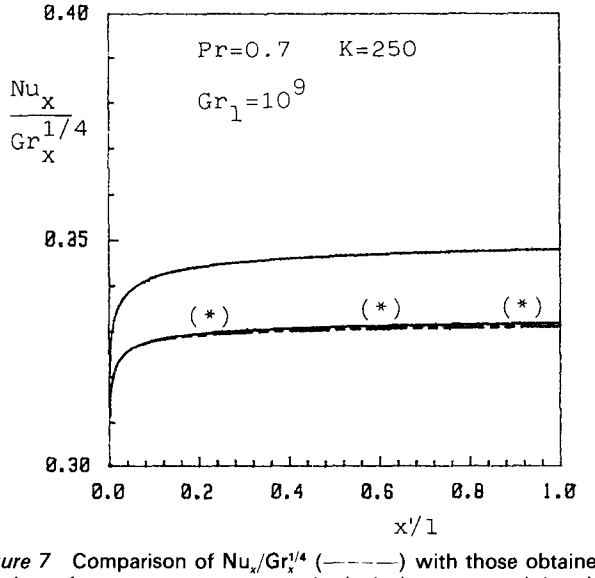


*Figure 7* Comparison of $Nu_x/Gr_x^{1/4}$ (————) with those obtained by the reference temperature method, (*) curve, and by the approximation $\mu\rho=\lambda\rho=1$

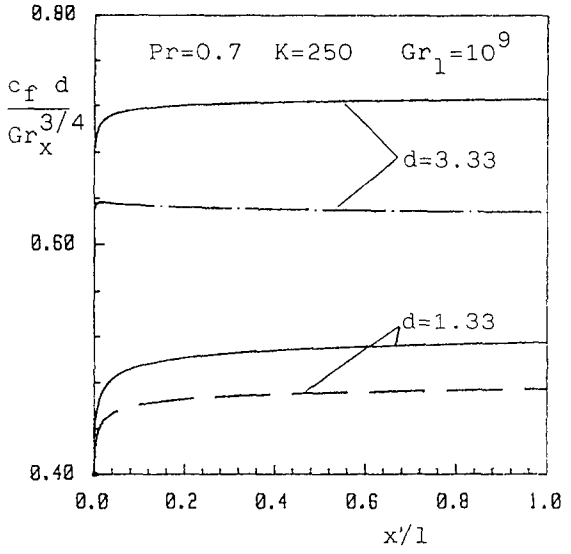


*Figure 8* Comparison of $c_f d/Gr_x^{3/4}$ for $d=1.33$ and $d=3.33$ with that of $\mu\rho=\lambda\rho=1$

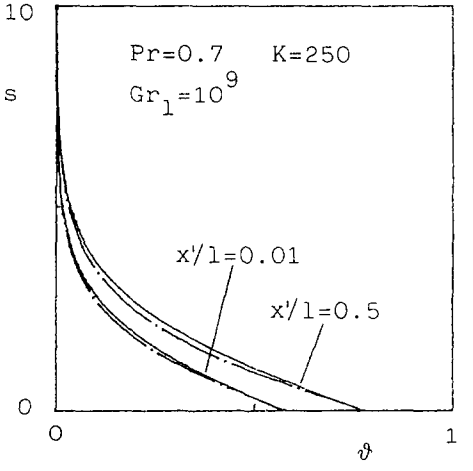


*Figure 9* Plot of nondimensional temperature $\vartheta$ versus $s=\eta/(px)^{1/5}$ for $d=3.33$

Figures 9 and 10 present dimensionless temperature and velocity profiles ($s=\eta/(px)^{1/5}$, the similarity variable for the initial expansion) for $K=250$ and $T_b=1300$ K. Figures 9 and 10 show that the approximation $\mu\rho=\lambda\rho=1$ is acceptable for the temperature ranges considered.

We summarize the preceding results in Table 1 by presenting some significant quantities obtained from the isothermal solution. All of the results apply to the case of air and are based on the assumptions that $T_\infty=300$ K, $T_b=700$, 1000, and 1300 K, and Pr = 0.7. For different gases and for different ranges of temperature, the values of the coefficients $a_1$ and $b_1$, appearing in the dimensionless products $\mu\rho$ and $\lambda\rho$ (Equations 7a and 8a) will be different. To analyze the influence of $a_1$ and $b_1$ on the thermo-fluid-dynamic field, we plotted in Figures 11 and 12 the curves of $Nu_x/Gr_x^{1/4}$ and $(1+d)c_f/Gr_x^{3/4}$ versus $b_1$ for several values of $a_1$ for isothermal boundary conditions, assuming that Pr = 0.7. Both nondimensional groups vary almost linearly with $a_1$ and $b_1$ in the ranges considered.

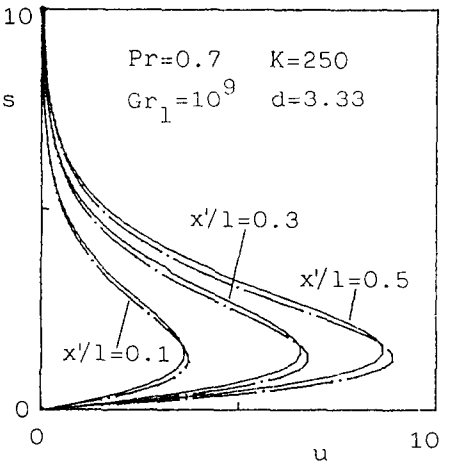


*Figure 10* Plot of nondimensional velocity component $u$ versus $s=\eta/(px)^{1/5}$ for $d=3.33$

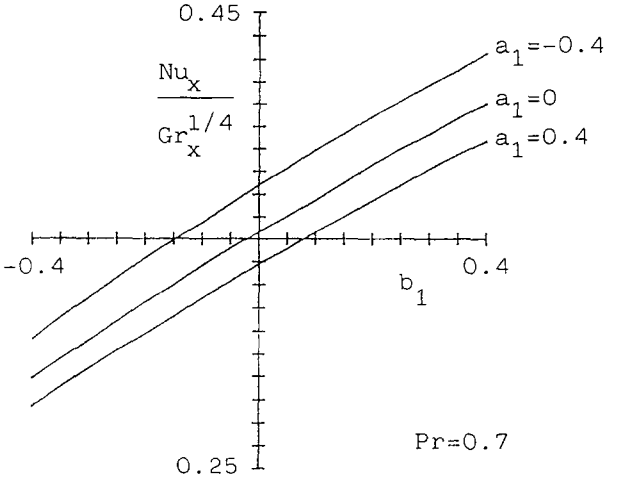


*Figure 11* Plot of $Nu_x/Gr_x^{1/4}$ for the isothermal solution versus $b_1$ for $a_1=-0.4$, 0, and 0.4 (Pr = 0.7)

## Conclusions

We analyzed the variable-property effects in laminar convection along a vertical flat plate of nonzero thickness. In order to study these effects, we assumed that $\mu(T)$ and $\lambda(T)$ can be represented by functions of the form $\sum_{i=1}^{n}\alpha_i T^i$. We further assumed that $n=2$ for air in the temperature range 300–1300 K, which proved to be sufficient.

**Table 1** Quantities obtained from the isothermal solution for $T_\infty=300$ K

| | $a_1$ | $b_1$ | $f_0''$ | $\vartheta_0'$ | $Nu_x/Gr_x^{1/4}$ | $(1+d)c$ |
|---|---|---|---|---|---|---|
| $\mu\rho=\lambda\rho=1$ | 0 | 0 | 0.960 | −0.353 | 0.353 | 0.960 |
| $T_b=700$ K | −0.229 | −0.177 | 1.120 | −0.408 | 0.336 | 0.864 |
| $T_b=1000$ K | −0.316 | −0.228 | 1.206 | −0.430 | 0.332 | 0.825 |
| $T_b=1300$ K | −0.380 | −0.267 | 1.283 | −0.449 | 0.329 | 0.796 |

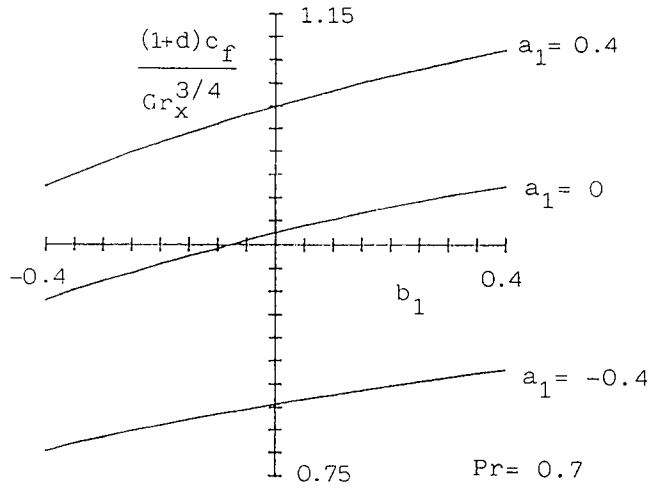


*Figure 12* Plot of $(1+d)c_f/Gr_x^{3/4}$ for the isothermal solution versus $b_1$ for $a_1 = -0.4$, 0, and 0.4 (Pr = 0.7)

The problem, which does not allow the use of similarity solutions, was solved by means of two expansions—initial and asymptotic—extending a method previously used by the authors.[10] In fact, in the present study we showed that the Padé-approximants technique can be used not only for calculating the radius of convergence of the initial expansion but also for representing the unknowns of the problem in the entire thermo-fluid-dynamic field.

The results show that, for air in the temperature ranges considered, the approximation $\mu\rho = \lambda\rho = 1$ works well enough, but not all quantities of interest can be calculated with the same accuracy; for example, the error was greater than 10% for the friction coefficient but less than 10% for the Nusselt number.

These results do not hold when the dependence of $\mu$ and $\lambda$ on $T$ is stronger than that shown for air in the ranges considered. In fact, the analysis proved that $c_f$ and Nu depend almost linearly on the coefficients $a_1$ and $b_1$ that represent the variation law of $\mu(T)$ and $\lambda(T)$.

## Acknowledgment

This work was supported by Ministero Pubblica Istruzione.

## References

1 Kays, W. M. *Convective Heat and Mass Transfer*. McGraw-Hill, New York, 1966

2 Sparrow, E. M. and Gregg, J. L. The variable fluid property problem in free convection. *Trans. Am. Soc. Mech. Engrs.*, 1958, **80**, 869–886

3 Minkowycz, W. J. and Sparrow, E. M. Free convection heat transfer to steam under variable property conditions. *Int. J. Heat Mass Transfer*, 1966, **9**, 1145–1147

4 Fujii, T., Takeuchi, M., Fujii, M., Suzaki, K., and Uehara, H. Experiments on natural heat transfer from the outer surface of a vertical cylinder to liquids. *Int. J. Heat Mass Transfer*, 1970, **13**, 753–787

5 Carey, V. P. and Mollendorf, J. C. Variable viscosity effects in several natural convection flows. *Int. J. Heat Mass Transfer*, 1980, **23**, 95–109

6 Gray, D. D. and Giorgini, A. The validity of the Boussinesq approximation for liquids and gases. *Int. J. Heat Mass Transfer*, 1976, **19**, 545–551

7 Merker, G. P. and Mey, S. Free convection in a shallow cavity with variable properties—1. Newtonian fluid. *Int. J. Heat Mass Transfer*, 1987, **30**, 1825–1832

8 Herwig, H. The effect of variable properties on momentum and heat transfer in a tube with constant heat flux across the wall. *Int. J. Heat Mass Transfer*, 1985, **28**, 423–431

9 Herwig, H. and Klemp, K. Variable property effects of fully developed laminar flow in concentric annuli. *J. Heat Transfer*, 1988, **110**, 314–320

10 Pozzi, A. and Lupo, M. The coupling of conduction with laminar natural convection along a flat plate. *Int. J. Heat Mass Transfer*, 1988, **31**, 1807–1814

11 *Handbook of Chemistry and Physics*. CRC Press, Boca Raton, FL, 1986